



# Kinetic optimisation of the reversed phase liquid chromatographic separation of rooibos tea (*Aspalathus linearis*) phenolics on conventional high performance liquid chromatographic instrumentation

Theresa Beelders<sup>a</sup>, Gunnar O. Sigge<sup>a</sup>, Elizabeth Joubert<sup>a,b</sup>, Dalene de Beer<sup>b</sup>, André de Villiers<sup>c,\*</sup>

<sup>a</sup> Department of Food Science, Stellenbosch University, Private Bag X1, Matieland 7602, South Africa

<sup>b</sup> Post-Harvest and Wine Technology Division, ARC Infruitec-Nietvoorbij, Private Bag X5026, Stellenbosch 7599, South Africa

<sup>c</sup> Department of Chemistry and Polymer Science, Stellenbosch University, Private Bag X1, Matieland 7602, South Africa

## ARTICLE INFO

### Article history:

Received 17 August 2011

Received in revised form 1 November 2011

Accepted 6 November 2011

Available online 12 November 2011

### Keywords:

Rooibos tea

Phenolic compounds

High performance liquid chromatography

Kinetic plots

Mass spectrometry

## ABSTRACT

Rooibos tea, produced from the endemic South African shrub *Aspalathus linearis*, has various health-promoting benefits which are attributed to its phenolic composition. Generating reliable, quantitative data on these phenolic constituents is the first step towards documenting the protective effects associated with rooibos tea consumption. Reversed phase liquid chromatographic (RP-LC) methods currently employed in the quantitative analysis of rooibos are, however, hampered by limited resolution and/or excessive analysis times. In order to overcome these limitations, a systematic approach towards optimising the RP-LC separation of the 15 principal rooibos tea phenolics on a 1.8  $\mu\text{m}$  phase using conventional HPLC instrumentation was adopted. Kinetic plots were used to obtain the optimal configuration for the separation of the target analytes within reasonable analysis times. Simultaneous optimisation of temperature and gradient conditions provided complete separation of these rooibos phenolics on a 1.8  $\mu\text{m}$  C18 phase within 37 min. The optimised HPLC-DAD method was validated and successfully applied in the quantitative analysis of aqueous infusions of unfermented and fermented rooibos. Major phenolic constituents of fermented rooibos were found to be a phenylpropanoid phenylpyruvic acid glucoside (PPAG), the dihydrochalcone C-glycoside aspalathin, the flavones isoorientin and orientin, and a flavonol O-diglycoside tentatively identified as quercetin-3-O-robinobioside. Content values for PPAG, ferulic acid and quercetin-3-O-robinobioside in rooibos are reported here for the first time. Mass spectrometric (MS) and tandem MS detection were used to tentatively identify 13 additional phenolic compounds in rooibos infusions, including a new luteolin-6-C-pentoside-8-C-hexoside and a novel C-8-hexosyl derivative of aspalathin reported here for the first time.

© 2011 Elsevier B.V. All rights reserved.

## 1. Introduction

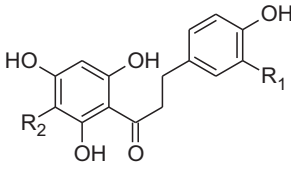
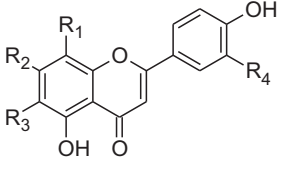
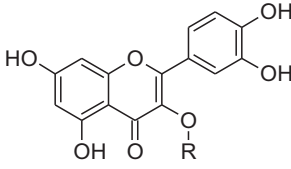
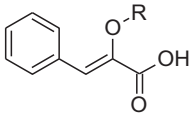
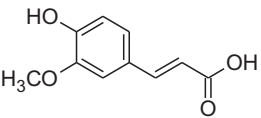
Rooibos (*Aspalathus linearis*) is a leguminous shrub endemic to the Western Cape Province in South Africa. Herbal tea is prepared from both the unfermented “green” and fermented “oxidised” plant material, although consumption of the traditional fermented product is more common and has a long history of use. In less than 20 years the international market demand for rooibos steadily grew from 750 tons in 1993 to 5633 tons in 2010. This increase has coincided with the interest of consumers in natural antioxidants as rooibos gained prominence as an antioxidant-containing beverage with potential health-promoting benefits. It has also led to value-added rooibos products such as extracts for the supplement/nutraceutical and functional food markets [1].

The secondary metabolites previously identified in fermented *A. linearis* plant material include single ring phenolic acids and monomeric flavonoids such as dihydrochalcones, flavanones, flavones, and flavonols [2]. In addition, recently the presence of phenolic compounds such as di-C-glycosyl flavones has been established in rooibos by LC-MS [3–5]. Quantitative data on the phenolic constituents of rooibos are essential to understand their role as potential bioactives. However, insufficient data on the dietary exposure to rooibos flavonoids are currently available [6]. Quantitative data on the rooibos phenolic compounds are either limited to a few of the major compounds such as aspalathin, nothofagin and their corresponding flavones, or to a limited number of samples, which do not reflect the natural variation.

Reversed phase liquid chromatography (RP-LC) is commonly used for the analysis of rooibos infusions. However, RP-LC methods currently employed in the quantitative analysis of rooibos are hampered by limited resolution and/or excessive analysis times [3,4,6–11]. These methods typically employ 5.0  $\mu\text{m}$  phases and are

\* Corresponding author. Tel.: +27 21 808 3351; fax: +27 21 808 3361.  
E-mail address: [ajdevill@sun.ac.za](mailto:ajdevill@sun.ac.za) (A. de Villiers).

**Table 1**  
Structures of the principal rooibos phenolic compounds.

General structure	No. <sup>a</sup>	Phenolic compound	Substituents
	4 12	<i>Dihydrochalcones</i> Aspalathin Nothofagin	R <sub>1</sub> = OH, R <sub>2</sub> = C-β-D-glucosyl R <sub>1</sub> = H, R <sub>2</sub> = C-β-D-glucosyl
	3 2 6 9 14 11 15	<i>Flavones</i> Orientin Isoorientin Vitexin Isovitexin Luteolin Luteolin-7-O-glucoside Chrysoeriol	R <sub>1</sub> = C-β-D-glucosyl, R <sub>2</sub> = R <sub>4</sub> = OH, R <sub>3</sub> = H R <sub>1</sub> = H, R <sub>2</sub> = R <sub>4</sub> = OH, R <sub>3</sub> = C-β-D-glucosyl R <sub>1</sub> = C-β-D-glucosyl, R <sub>2</sub> = OH, R <sub>3</sub> = R <sub>4</sub> = H R <sub>1</sub> = R <sub>4</sub> = H, R <sub>2</sub> = OH, R <sub>3</sub> = C-β-D-glucosyl R <sub>1</sub> = R <sub>3</sub> = H, R <sub>2</sub> = R <sub>4</sub> = OH R <sub>1</sub> = R <sub>3</sub> = H, R <sub>2</sub> = O-β-D-glucosyl, R <sub>4</sub> = OH R <sub>1</sub> = R <sub>3</sub> = H, R <sub>2</sub> = OH, R <sub>4</sub> = OCH <sub>3</sub>
	13 10 7 8	<i>Flavonols</i> Quercetin Isoquercitrin Hyperoside Rutin	R = H R = O-β-D-glucosyl R = O-β-D-galactosyl R = O-β-D-rutinosyl
	1	<i>Phenylpropanoid</i> Phenylpyruvic acid-2-O-glucoside (PPAG)	R = O-glucosyl
	5	<i>Hydroxycinnamic acid</i> Ferulic acid	

<sup>a</sup> According to RP-LC retention times (Fig. 5).

only suitable for the quantification of some of the major phenolic compounds in analysis times up to 125 min, restricting their suitability for routine application.

Recent developments in LC may be used to improve conventional methods for phenolic analysis [12]. Of these, particularly the use of columns packed with sub-2 μm particles operated at elevated temperatures provides an attractive alternative for the fast and efficient analysis of rooibos phenolics using conventional instrumentation. Iswaldi and co-workers [5] recently presented a qualitative method on the analysis of rooibos phenolics utilizing a column with 1.8 μm particles, although this method was not optimised for the separation of the most important compounds. Cabooter and co-workers [13] recently reported a method for the separation of the principal rooibos phenolics on a 200 mm long column packed with 1.7 μm particles operated at 1000 bar. However, such ultra high pressure liquid chromatography (UHPLC) instrumentation is not commonly available in laboratories charged with routine analysis of rooibos.

In light of the above, the aim of the current paper was to develop a RP-LC method on a sub-2 μm particle phase suitable for the fast, routine quantification of the most important rooibos phenolics (Table 1) on conventional HPLC instrumentation. The kinetic benefits of this phase compared to conventional RP-LC phases were evaluated, followed by the systematic optimisation of gradient conditions to allow separation of the target analytes within a reasonable analysis time. The optimised method was applied to the analysis of aqueous infusions prepared from unfermented and

fermented rooibos plant material, and high resolution mass spectrometry and tandem mass spectrometry were used to confirm peak purity and identify additional phenolic compounds present in each of these samples.

## 2. Experimental

### 2.1. Chemicals and columns

HPLC gradient-grade acetonitrile was purchased from Merck (Darmstadt, Germany), methanol from Riedel-de Haën (Sigma-Aldrich, St. Louis, MO, USA) and acetic acid from Fluka (Sigma-Aldrich, Johannesburg, South Africa). Deionised water, prepared using a Modulab (Continental Water Systems Corporation, San Antonio, TX, USA) water purification system, was further purified to HPLC-grade using a Milli-Q academic (Millipore, Milford, MA, USA) water purification system. Acetophenone and uracil were obtained from Fluka, while phenolic standards (Table 1) were from Extrasynthese (Genay Cedex, France), Roth (Karlsruhe, Germany), Sigma-Aldrich and Fluka. Enolic phenylpyruvic acid-2-O-glucoside (PPAG) was isolated and supplied by the Post-Harvest & Wine Technology Division of the Agricultural Research Council of South Africa (ARC Infruitec-Nietvoorbij, Stellenbosch, South Africa). Aspalathin and nothofagin were supplied by the PROMEC Unit of the Medical Research Council of South Africa (Cape Town, South Africa). Stock solutions of the phenolic standards were prepared in dimethyl sulfoxide (Fluka) at concentrations of approximately 1 mg/mL and diluted with water according to experimental

requirements. All diluted solutions contained 0.5 mg/mL ascorbic acid (Sigma) and were filtered through 0.22  $\mu\text{m}$  hydrophilic PVDF filters (Millipore) prior to use.

The following 4.6 mm i.d. columns were employed in this study: a 150 mm 5.0  $\mu\text{m}$   $d_p$  Phenomenex Gemini C18 column (Torrance, LA, USA); and 50 mm and 100 mm 1.8  $\mu\text{m}$   $d_p$  Agilent Zorbax SB-C18 columns (Agilent Technologies, Waldbronn, Germany).

## 2.2. Preparation of aqueous rooibos infusions

Randomly selected samples of unfermented ( $n=10$ ) and fermented ( $n=10$ ) rooibos plant material were obtained from South Africa. Duplicate infusions were prepared by infusing 2.5 g plant material for 5 min with 200 mL freshly boiled deionised water without agitation. The infusions were decanted through a tea strainer, filtered through Whatman No. 4 filter paper and cooled to room temperature. The soluble solid contents of the infusions were determined in 20 mL aliquots using a gravimetric method. Aliquots (ca. 1.5 mL) were stored at  $-20^\circ\text{C}$  until analysis. For LC analyses, aliquots of the rooibos infusions were thawed at room temperature and filtered through 0.22  $\mu\text{m}$  hydrophilic PVDF filters. Subsequently 1 mL of the filtrate was pipetted into a 1.5 mL amber autosampler vial and 100  $\mu\text{L}$  10% ascorbic acid in water (v/v) added. All samples were analysed within 24 h of sample preparation.

## 2.3. Instrumentation

All analyses were performed using a mobile phase consisting of (A) 2% acetic acid in water (v/v) and (B) acetonitrile. HPLC analyses were conducted on an Agilent 1200 series instrument (maximum pressure 400 bar) equipped with an in-line degasser, quaternary pump, autosampler, column thermostat and diode-array detector (standard 13  $\mu\text{L}$  flow cell, 10 mm path length) controlled by Chemstation software (all from Agilent Technologies). The dwell volume of this system was measured as 0.82 mL.

UHPLC analyses were conducted on an Acquity UPLC system (using a maximum pressure of 400 bar) equipped with a binary solvent manager, sample manager, column heating compartment and photodiode-array (PDA) detector (Waters, Milford, MA, USA). The detector was equipped with a 500 nL flow cell (10 mm path length). The dwell volume of this system was 0.07 mL.

High resolution LC-MS analyses were conducted on a UPLC-Synapt GT Q-TOF system (Waters) equipped with a PDA.

## 2.4. Chromatographic conditions

### 2.4.1. Construction of kinetic plots

For HPLC analyses on the Gemini column ( $25^\circ\text{C}$ ), the external volume of the system was minimised by using minimal lengths of 0.13 mm i.d. PEEK tubing. 10  $\mu\text{L}$  injections were performed (100  $\mu\text{L}$  injection loop). For UHPLC analyses on the 50 mm Zorbax column ( $25$  and  $50^\circ\text{C}$ ), injections were performed in the full loop mode (5  $\mu\text{L}$  injection loop) using mobile phase A as weak needle wash solvent.

Phenolic compounds and acetophenone were diluted in the mobile phase, together with uracil as unretained marker. Concentrations ranged between 2.5 and 12.5 mg/L. The organic content of the mobile phase was adjusted to yield constant retention factors for each of the analytes on the different stationary phases and at different temperatures. Plate height measurements were performed in isocratic mode by systematically increasing the flow rate from 0.1 mL/min in increments of 0.1 mL/min until the maximum column pressure was reached (in the case of the Zorbax column up to a maximum flow rate of 2 mL/min). UV detection was performed at 288 nm.

All experimental values represent the average of three measurements and were obtained after correction for the extra-column

band broadening ( $\sigma_{\text{extra}}^2$ ),  $t_0$ -time ( $t_{\text{extra}}$ ) and pressure drop ( $\Delta P_{\text{extra}}$ ). The extra-column peak variance for the Agilent 1200 series instrument ranged between 0.26 and 14 s<sup>2</sup> (for flow rates 2.6–0.1 mL/min), resulting in 0.10–1.7% losses in efficiency on the Gemini column. For the Acquity UPLC system  $\sigma_{\text{extra}}^2$  ranged between 0.027 and 7.0 s<sup>2</sup> (flow rate 2.0–0.1 mL/min), leading to losses in efficiency of 0.0–1.4% on the 50 mm Zorbax column. For the construction of plate height curves, the number of theoretical plates ( $N$ ) was calculated using the peak width at half height obtained from Agilent Chemstation software. The retention time of uracil ( $t_0$ ) was used to calculate linear velocity ( $u_0$ ) and retention factors ( $k$ ). Kinetic plots were constructed using a freely downloadable spreadsheet template [14]. Mobile phase viscosity ( $\eta$ , Pa s) was calculated using water/acetonitrile as the mobile phases according to Guillaume et al. [15], while diffusion coefficients ( $D_M$ , m<sup>2</sup>/s) were calculated using the Wilke–Chang equation [16]. Column permeabilities ( $K_V$ , m<sup>2</sup>) were determined using the general pressure drop equation [17]. For the maximum pressure ( $\Delta P_{\text{max}}$ ), values of 240 and 400 bar were used for the Gemini and Zorbax columns, respectively.

### 2.4.2. Evaluation of mobile phase composition and temperature

Optimisation experiments were conducted on the Agilent 1200 system with UV detection at 288 nm using the standards and uracil diluted in the mobile phase. Experimental data were generated in isocratic mode on the 100 mm Zorbax column protected with an Acquity UPLC in-line filter (Waters) at a flow rate of 0.8 mL/min.

The effect of solvent strength was investigated by systematically increasing the volume fraction of the organic modifier ( $\varphi$ ) from 0.075 to 0.400 in increments of 0.025. The column was thermostatted at  $25^\circ\text{C}$  throughout. For the construction of Van't Hoff plots, the column temperature was systematically increased from 25 to  $60^\circ\text{C}$  in increments of  $5^\circ\text{C}$ . The mobile phase composition was varied to obtain retention factors ranging between 5 and 50. Values represent the average of three measurements.

### 2.4.3. Optimised HPLC–DAD method for routine analysis

Routine analyses were performed on the Agilent 1200 system at  $37^\circ\text{C}$  using the 100 mm Zorbax column protected with an Acquity UPLC in-line filter and a 5.0  $\mu\text{m}$  SB-C18 guard column (Agilent). An injection volume of 50  $\mu\text{L}$  was used for all fermented rooibos infusions, while the injection volume for the unfermented rooibos infusions was adjusted to provide a response for aspalathin within the linear range. The flow rate was 1.0 mL/min and a multilinear gradient was performed as follows: 10% B (0–2 min), 10–14.8% B (2–19 min), 14.8–36.8% B (19–34 min), 36.8–100% B (34–37 min), 100% B isocratic (37–42 min), 100–10% B (42–45 min). The column was re-equilibrated for 5 min. UV spectra were recorded between 200–700 nm with selective wavelength monitoring at 288 and 350 nm.

Preliminary validation was performed in terms of linearity, intra- and interday analytical precision as well as analyte stability [18]. The dihydrochalcones and PPAG were quantified at 288 nm, while the flavones, flavonols and ferulic acid were quantified at 350 nm. Quercetin-3-*O*-robinobioside was quantified using the calibration curve for rutin (quercetin-3-*O*-rutinoside) since no standard was available for this compound. Calibration mixtures were injected at nine different injection volumes corresponding to 0.025–1.2  $\mu\text{g}$  on-column, covering the concentration ranges of the compounds in aqueous rooibos infusions. Linear regression was performed for each compound to determine the slope,  $y$ -intercept and correlation coefficients ( $r^2$ ).

### 2.4.4. Comparative HPLC–DAD methods for routine analysis

For comparative quantitative analyses, the method reported in [6] was used for the quantification of PPAG, isoorientin, orientin,

aspalathin, rutin and nothofagin. An adapted method from [7] was used for the quantification of vitexin, isovitexin, luteolin-7-O-glucoside, hyperoside, quercetin, luteolin and chrysoeriol. Adjustments to the method of [7] led to the following chromatographic conditions: Analyses performed at 38 °C using the 150 mm Gemini column protected with a Gemini C18 guard cartridge (4 mm × 3 mm). The flow rate was 0.4 mL/min and the binary mobile phase consisted of (A) 2% acetic acid in water (v/v) and (B) methanol. A multilinear gradient was performed as follows: 20% B (0–3 min), 20–30% B (3–15 min), 30% B (15–18 min), 30–35% B (18–27 min), 35% B (27–29 min), 35–40% B (29–35 min), 40–60% B (35–54 min), 60–80% B (54–62 min), 80–60% B (62–68 min), 60–20% B (68–81 min). The column was re-equilibrated for 9 min at a flow rate of 1.2 mL/min. All analyses were performed on the Agilent 1200 system.

#### 2.4.5. LC-ESI-MS and LC-ESI-MS/MS analyses

UPLC-ESI-MS and MS/MS analyses were performed as outlined in Section 2.4.3, except that the in-line filter was replaced by the Acquity Column Stabilizer (Waters) and an analysis temperature of 38 °C was used. Data were acquired in the high resolution (150–1500 amu) and MS/MS scanning modes and processed using MassLynx v.4.1 software (Waters). The instrument was operated in positive and negative ionisation modes and calibrated using a sodium formate solution. Leucine encaphalin was used for lock-spray. The capillary voltage was 3.0 and –3.5 kV in positive and negative ionisation modes, respectively, and the sampling cone voltage was 20.0 V. The source temperature was 120 °C, while desolvation temperature was set at 350 °C. Desolvation gas flow (N<sub>2</sub>) was 500 L/h and cone gas flow (N<sub>2</sub>) 50 L/h. For MS/MS experiments, a trap collision energy of 30 V was used. The rest of the parameters were optimised for best sensitivity. The eluent was split 3:2 prior to introduction into the ionisation chamber. Injection volumes of 5 and 10 µL were used for the standard mixture and aqueous rooibos infusions, respectively. Injections were performed in the partial loop mode (10 µL injection loop) with 20% MeOH in water (v/v) as weak needle wash solvent. PDA data were acquired over a wavelength range of 220–400 nm at a sampling rate of 10 points/s.

### 3. Results and discussion

In order to develop a single method suitable for the fast, simultaneous quantification of the major rooibos phenolics on conventional instrumentation, a systematic approach towards optimising separation on a 1.8 µm RP-LC column was adopted. This entailed kinetic evaluation of this phase, followed by simultaneous optimisation of the gradient profile and temperature.

#### 3.1. Kinetic evaluation of the effect of stationary phase particle size and temperature on the separation of rooibos phenolics

A 1.8 µm column was selected for this study due to the known benefits of such phases for speeding up routine RP-LC analyses [19]. Moreover, column lengths up to 100 mm of this phase may be used on conventional instrumentation to provide separations of the same efficiency as obtained on conventional (250 mm, 5.0 µm) phases. The mobile phase selected consisted of (A) 2% acetic acid in water (v/v) and (B) acetonitrile. The slightly acidified aqueous phase is required to suppress ionisation [20], while the selection of acetonitrile as organic modifier, as opposed to methanol, was based primarily on lower viscosity (*i.e.* lower operating pressure) and, to a lesser extent, on selectivity considerations.

The 1.8 µm phase was kinetically evaluated at two different temperatures (25 and 50 °C) and compared to a conventional 5.0 µm column, thermostatted at 25 °C. The potential benefits provided by this strategy for improved separation of rooibos phenolics

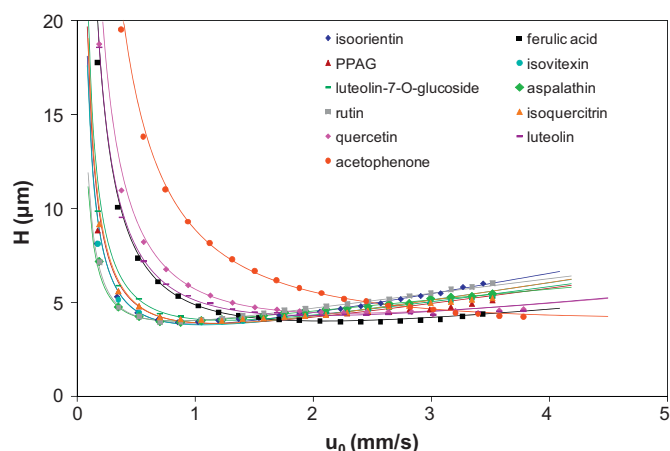


**Fig. 1.** Van Deemter curves obtained for selected rooibos phenolic compounds and acetophenone on an Agilent Zorbax SB-C18 column (50 mm × 4.6 mm, 1.8 µm  $d_p$ ), thermostatted at 25 °C. For a summary of the plate height results, refer to Table 2.

were determined by constructing van Deemter curves and kinetic plots [14] for these compounds. Plate height curves were measured on a 50 mm 1.8 µm column in order to obtain the maximum number of data points in the C-term regime. Note that although the final method optimisation was performed on a 100 mm column of the same phase, it has been shown practically [21] that extrapolation of kinetic performance data for a particular phase to longer column lengths remains valid.

Studies used to assess the kinetic benefits provided by small particle-packed columns typically use common organic molecules such as acetophenone as test analytes, since these compounds exhibit ideal thermodynamic behaviour [22]. Various authors have, however, reported significant differences in the plate height behaviour of such test analytes in comparison with real-life compounds [17,22,23]. While limited kinetic data on phenolic compounds have been reported [12], it is to be expected that these relatively large, structurally diverse molecules will exhibit dissimilar plate height behaviour. Therefore, in the first instance, the kinetic behaviour of rooibos phenolics was investigated relative to acetophenone. Experimental plate height data obtained on a 1.8 µm column thermostatted at 25 °C are illustrated in Fig. 1. Relevant data for these van Deemter curves are summarised in Table 2.

**Table 2**

Summary of plate height data obtained for selected rooibos phenolic compounds and acetophenone on an Agilent Zorbax SB-C18 column (50 × 4.6 mm, 1.8 µm  $d_p$ ) at 25 °C.

Compound	$D_M$ (m <sup>2</sup> /s)	$k$	$H_{min}$ (µm)	$u_{opt}$ (mm/s)
Acetophenone	$7.99 \times 10^{-10}$ a	7.08	4.25 <sup>b</sup>	4.49 <sup>b</sup>
Aspalathin	$3.89 \times 10^{-10}$ c	3.84	4.00	0.84
Isoorientin	$3.94 \times 10^{-10}$ d	5.29	3.85	1.01
Isovitexin	$3.99 \times 10^{-10}$ c	5.34	3.80	1.08
Luteolin	$5.32 \times 10^{-10}$ a	6.21	4.30	2.05
Luteolin-7-O-glucoside	$3.93 \times 10^{-10}$ c	6.78	4.05	1.25
Quercetin	$5.23 \times 10^{-10}$ a	6.42	4.41	2.27
Isoquercitrin	$3.89 \times 10^{-10}$ c	6.55	3.88	1.17
Rutin	$3.24 \times 10^{-10}$ c	5.23	4.03	0.84
PPAG	$4.53 \times 10^{-10}$ c	3.36	3.91	1.16
Ferulic acid	$6.17 \times 10^{-10}$ d	8.66	4.00	2.11

<sup>a</sup> Calculated according to the Wilke–Chang equation [16] using a mobile phase composition of 25/75 acetonitrile/2% acetic acid in water (v/v).

<sup>b</sup> Extrapolated from experimental data acquired up to 3.79 mm/s.

<sup>c</sup> Calculated as for footnote 'a' using a mobile phase composition of 15/85 acetonitrile/2% acetic acid in water (v/v).

<sup>d</sup> Calculated as for footnote 'a' using a mobile phase composition of 12.5/87.5 acetonitrile/2% acetic acid in water (v/v).



These results were obtained using the same experimental configuration (instrument, column and temperature), and therefore variations in the shape of the van Deemter curves can primarily be attributed to the physicochemical properties of the analytes. Differences in analyte retention ( $k$ , Table 2) influence both the  $B$ - and the  $C$ -terms of the van Deemter equation [17]. For this reason, the mobile phase composition was adjusted experimentally to limit  $k$  between 3 and 10, and therefore the contribution of this factor can be considered as negligible.

Experimental data (Table 2) indicate that the minimum plate heights, and hence the maximum efficiencies attainable for a given column length, are approximately similar for all compounds. The slightly higher  $H_{\min}$  values obtained for acetophenone, luteolin and quercetin can presumably be attributed to the combined effect of slightly higher  $k$  values and the use of a less viscous mobile phase.

Significant differences were observed in the optimal linear velocity ( $u_{\text{opt}}$ ) between all compounds. Isoorientin, isovitexin, luteolin-7-*O*-glucoside, isoquercitrin, and PPAG are characterised by optimal linear velocities ranging between 1.0 and 1.2 mm/s, while  $u_{\text{opt}}$  values for luteolin, quercetin and ferulic acid are comparable at 2.0–2.2 mm/s (Table 2). Rutin and aspalathin have extremely low optimal linear velocities equal to 0.84 mm/s, whereas this value is significantly higher for the test analyte, acetophenone ( $u_{\text{opt}} = 4.49$  mm/s, extrapolated). Practically, this implies that the optimal flow rate for aspalathin is approximately 0.5 mL/min (on a 4.6 mm i.d. column) and hence operating this column at conventional flow-rates of 1.0–1.5 mL/min will result in an efficiency loss of up to 20%. The relatively low optimal flow rates for the phenolics on the 4.6 mm i.d. 1.8  $\mu\text{m}$  column (0.48–1.20 mL/min) imply that analyses under optimal conditions may be performed on conventional instrumentation with maximum operating pressures of 400 bar. This is not the case for acetophenone, for which the optimal flow rate (2.38 mL/min) would correspond to an operating pressure of  $\sim 570$  bar for a 50 mm column length.

Variations in the shape of the experimental van Deemter curves can largely be ascribed to the different diffusion coefficients ( $D_M$ , Table 2) of the analytes under investigation. For compounds with lower  $D_M$  values, the  $B$ -term and  $C$ -term contributions to plate height are respectively smaller and larger, which together induce a significant reduction in the optimal linear velocity. For example, the optimal linear velocity for the flavonol aglycone, quercetin, was 2.27 mm/s, while the values for its monoglycosylated (isoquercitrin) and diglycosylated (rutin) derivatives were significantly lower at 1.17 and 0.84 mm/s, respectively. Considering the flavone phenolic subclass, a similar observation was made – the aglycone luteolin had an optimal linear velocity value of 2.05 mm/s, while its mono-*O*-glycoside (luteolin-7-*O*-glucoside) and mono-*C*-glycoside (isovitexin), had lower optimal linear velocities of 1.25 and 1.08 mm/s, respectively. It can therefore be concluded that, irrespective of the phenolic subclass and type of glycosidic bond ( $C-C$  vs  $C-O$ ), an increase in the degree of glycosylation (and hence molecular weight) leads to a decrease in the optimal linear velocity. In addition, an increase in the degree of glycosylation also results in a relatively steep increase in plate height in the  $C$ -term (high flow rate) regime. These results are in accordance with previous reports for large molecular weight analytes [17,22,24].

Further discussion on the effect of stationary phase particle size and temperature will be limited to aspalathin as representative compound since this is the principal phenolic constituent of rooibos tea. Moreover, since aspalathin also exhibits the most conservative plate height behaviour, kinetic optimisation for this compound relatively accurately reflects the performance of this column for rooibos analysis.

Current RP-LC methods employed in the quantitative analysis of rooibos typically use 5.0  $\mu\text{m}$  columns [4,6–9] operated at ambient [4,8,9] and moderately higher temperatures up to 40 °C

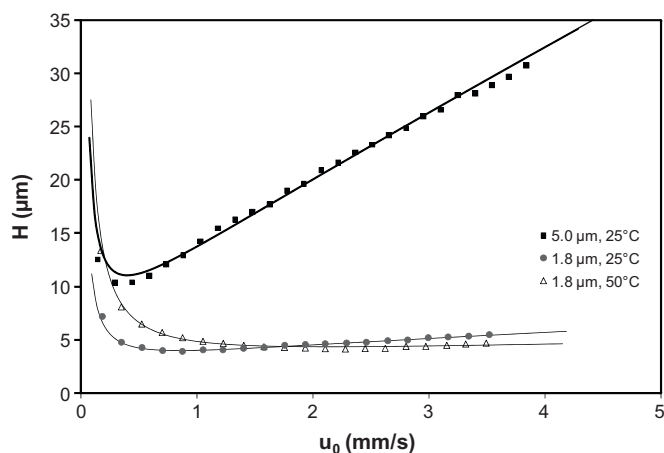


Fig. 2. Van Deemter curves obtained for aspalathin on a 5.0  $\mu\text{m}$  Phenomenex Gemini C18 column (150 mm  $\times$  4.6 mm) at 25 °C, and a 1.8  $\mu\text{m}$  Agilent Zorbax SB-C18 column (50 mm  $\times$  4.6 mm) at 25 and 50 °C.

[3,6,7,10,11]. Therefore a 5.0  $\mu\text{m}$  Phenomenex column operated at 25 °C was selected as reference in order to evaluate the kinetic benefits provided by the 1.8  $\mu\text{m}$  column. Plate height curves obtained for aspalathin on each of the investigated phases at the studied temperatures are illustrated in Fig. 2.

The minimum plate heights obtained for aspalathin on the 5.0  $\mu\text{m}$  and 1.8  $\mu\text{m}$  phases at 25 °C are 11.02 and 4.00  $\mu\text{m}$ , respectively, with corresponding  $u_{\text{opt}}$  values of 0.39 and 0.84 mm/s. As expected, a reduction in particle size resulted in an important reduction of the minimum plate height and an increase in the optimal linear velocity. Although not illustrated here, similar results were obtained for the other target phenolic compounds.

To evaluate the effect of temperature, a value of 50 °C was chosen to avoid the potential on-column degradation of the thermally labile phenolic compounds. With an increase in temperature (compare the 1.8  $\mu\text{m}$  phase at 25 and 50 °C, Fig. 2), the minimum plate height obtained for aspalathin remained virtually unaltered, while the optimum linear velocity was shifted towards a higher value (2.12 mm/s). This corresponds to an increase in the optimal flow rate from 0.48 to 1.22 mL/min on this column. This increase in optimal linear velocity is surprisingly large, considering that the calculated diffusion coefficient of aspalathin increases from  $3.9 \times 10^{-10}$  m<sup>2</sup>/s at 25 °C (Table 2) to  $6.0 \times 10^{-10}$  m<sup>2</sup>/s at 50 °C. We currently have no explanation for this larger-than-expected increase in optimal linear velocity. However, it is clear that the primary advantage afforded by operating at elevated temperature is a reduction in analysis time. Furthermore, the increase in temperature was accompanied by a decrease in the  $C$ -term [24], which may be exploited by applying higher flow rates to obtain fast separations without a significant loss in efficiency. This approach is, however, limited on conventional instrumentation with maximum pressure capabilities of 400 bar.

Kinetic plots were constructed according to Desmet et al. [14] using experimental data for the rooibos phenolics on the studied columns. Kinetic plots automatically yield the most relevant performance characteristics in terms of which experimental configuration will either yield faster separations for a required efficiency, or will achieve the maximum number of plates in a given analysis time.

Since the goal of this work was to develop a fast routine method for rooibos phenolics on conventional HPLC instrumentation, kinetic plots were constructed using a maximum pressure of 400 bar. These plots were used to compare the kinetic performance of the different supports for aspalathin. By manipulation of the experimental plate height data using the retention factor ( $k$ ),

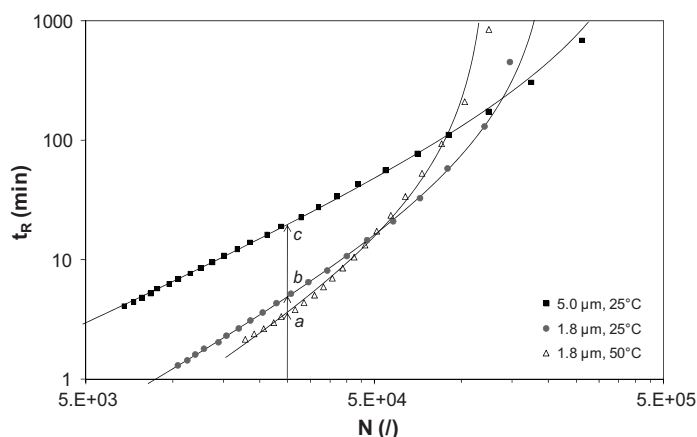


**Fig. 3.**  $t_R$  vs  $N$  plots obtained for aspalathin on a  $5.0\ \mu\text{m}$  Phenomenex Gemini C18 column ( $150\ \text{mm} \times 4.6\ \text{mm}$ ) at  $25\ ^\circ\text{C}$ , and a  $1.8\ \mu\text{m}$  Agilent Zorbax SB-C18 ( $50\ \text{mm} \times 4.6\ \text{mm}$ ) at  $25$  and  $50\ ^\circ\text{C}$ .

a plot of actual analysis time  $t_R$  vs  $N$  can be obtained [14] (Fig. 3). These plots yield the most sought-after kinetic data *i.e.*, the minimum analysis time needed to perform a separation requiring  $N$  plates.

Conventional routine HPLC methods for rooibos phenolics provide isocratic efficiencies of 15–25 000 plates. The latter value also roughly corresponds to the efficiency of a 100 mm  $1.8\ \mu\text{m}$  column (operated at optimal flow rate), the maximum length which may practically be used on conventional instrumentation at pressures up to 400 bar. Points *a–c* in Fig. 3 correspond to the analysis times for aspalathin that will provide a required efficiency of 25 000 plates. The analysis times obtained on the  $1.8\ \mu\text{m}$  phase thermostatted to  $50\ ^\circ\text{C}$  (point *a*) and  $25\ ^\circ\text{C}$  (point *b*), and on the  $5.0\ \mu\text{m}$  phase at  $25\ ^\circ\text{C}$  (point *c*), are approximately 4, 5 and 20 min, respectively. Therefore, for separations requiring 25 000 plates, a 75% decrease in analysis time can be obtained by switching to a smaller particle size, with a further 25% reduction obtained by increasing the temperature to  $50\ ^\circ\text{C}$ . Clearly, for analyses providing relatively low efficiencies such as typically used in routine HPLC methods, the use of smaller particle-packed columns operated at elevated temperature will provide much better performance.

Plots of  $t_0/N^2$  vs  $N$  for aspalathin are presented in Supplementary Information (Figure S1) to allow comparison of the range of efficiencies where each configuration provides optimal results in terms of the conventional kinetic plot representation.

### 3.2. Simultaneous optimisation of mobile phase composition and temperature

Having established the suitability of the  $1.8\ \mu\text{m}$  phase for fast, efficient separation of rooibos phenolics on conventional instrumentation, the effect of solvent strength and temperature on the retention behaviour of rooibos phenolics were investigated by constructing plots of  $\log k$  vs volume fraction of organic modifier ( $\phi$ ) and reciprocal temperature (Van't Hoff plots), for the 15 target analytes (Fig. 4).

Under isocratic elution conditions, analyte retention as a function of solvent strength ( $\phi=0.01\ \text{B}$ ) and temperature ( $T$ ) can be described by the following well-known relationships [25]:

$$\log k = \log k_W - S\phi$$

$$\log k = \frac{A+B}{T}$$

where  $k_W$  is the (extrapolated) value of  $k$  for  $\phi=0$  (water as mobile phase) and  $S$  is a constant for each analyte.  $A$  is a function of the

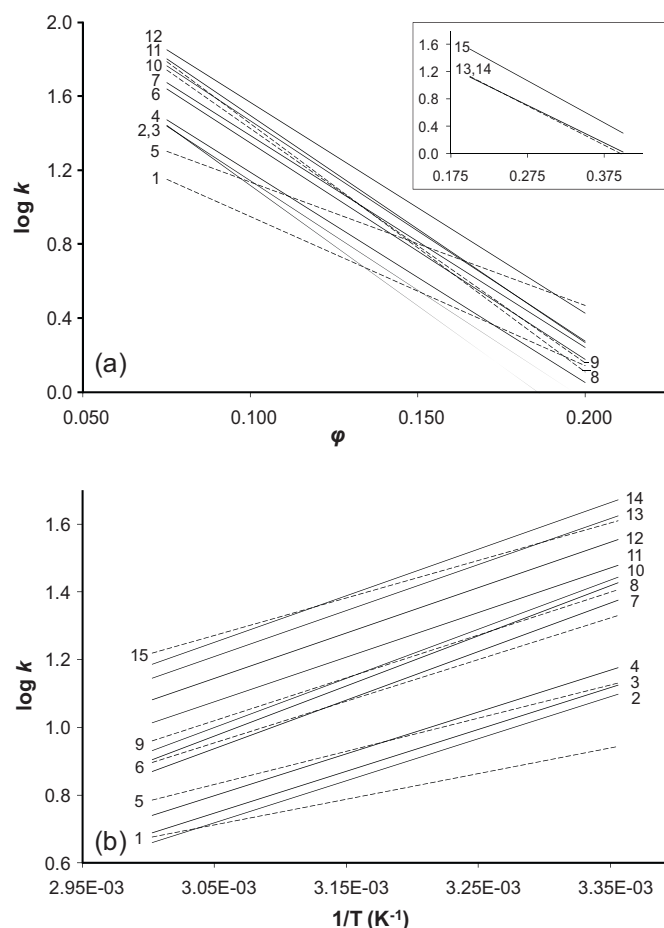


**Fig. 4.** (a) Plots of  $\log k$  vs volume fraction of organic modifier ( $\phi$ ) and (b) plots of  $\log k$  vs reciprocal temperature ( $\text{K}^{-1}$ ) for rooibos phenolics on the  $1.8\ \mu\text{m}$  Agilent Zorbax SB-C18 ( $100\ \text{mm} \times 4.6\ \text{mm}$ ) column. Data labels correspond to Table 1. The mobile phases consisted of 2% acetic acid (A) and acetonitrile (B). Note that for the more retained aglycones quercetin (13), luteolin (14) and chrysoeriol (15), the volume fraction of organic modifier was increased to 0.20–0.40 to obtain equivalent retention ( $2.0 < \log k < 0.0$ ) in (a).

phase ratio and entropy of retention,  $\Delta S$ , and  $B$  is proportional to the enthalpy of retention,  $\Delta H$ . Values of  $\Delta H$  are typically negative, so that retention decreases with increasing temperature [26] as observed for the phenolic standards (Fig. 4b).

The 15 rooibos phenolics represent an “irregular” sample, for which changes in solvent strength and temperature are associated with intersections of the individual curves and therefore retention order reversals [25]. Note specifically the behaviour of the non-flavonoid compounds PPAG (1) and ferulic acid (5) and the flavones vitexin (6), isovitexin (9) and chrysoeriol (15), for which the decrease in retention as a function of increasing temperature especially was less pronounced compared to the other compounds. The behaviour of the acidic compounds (1 and 5) may be explained by the effect of temperature on  $\text{pK}_a$  (increasing temperature leads to higher  $\text{pK}_a$ 's, and therefore lower ionisation) [27], although the reason for the unique behaviour of the flavones is unclear.

These data indicate that complete separation of all the compounds cannot be obtained under isocratic elution conditions. Selectivity effects as a function of changes in mobile phase composition and temperature in RP-LC are often complementary and therefore simultaneous optimisation of these two variables was used to improve resolution [27,28]. For this purpose, gradient runs were performed at two temperatures ( $25$  and  $60\ ^\circ\text{C}$ ) and two gradient times (5–50% B in 20 and 70 min). These data were used as

input for predictions based on computer simulations using DryLab software [29]. DryLab is based on the Linear Solvent Strength (LSS) theory and uses two gradient runs where only gradient time ( $t_G$ ) is varied to calculate values of  $S$  and  $k_W$  for each analyte. Although the prediction of retention times was sufficiently accurate, none of the simulated separations could provide baseline separation of the target phenolic compounds within acceptable pressures (results not shown). Important conclusions could however be drawn from the simulations to assist further experimental fine-tuning of the temperature and gradient.

Lower temperatures (23 °C) provided the best separation of the critical compounds **6–10**, with the apigenin-glycosides (vitexin and isovitexin) eluting before the quercetin-glycosides (hyperoside, rutin and isoquercitrin) in the elution order vitexin < isovitexin < hyperoside < rutin < isoquercitrin. However, at this temperature, pressure was excessive and perfect co-elution of quercetin and luteolin occurred, which could not be improved by manipulation of the gradient profile. As the temperature was systematically increased (gradient unchanged) the apigenin-glycosides were shifted towards higher retention times in comparison with the quercetin-glycosides, leading to the positioning of hyperoside and rutin between vitexin and isovitexin, while isoquercitrin eluted after isovitexin. This is in accordance with the isocratic retention data presented for these compounds as a function of temperature (Fig. 4b). The elution order at 37 °C was: vitexin < hyperoside < rutin < isovitexin < isoquercitrin. By further increasing the temperature, the apigenin-glycosides were more retained than the quercetin-glycosides, leading to perfect co-elution of vitexin + hyperoside and isovitexin + isoquercitrin. Hence the optimal column temperature was established at an intermediate temperature of 37 °C, where baseline separation of the two aglycones quercetin and luteolin could also be achieved.

An increase in gradient steepness (% B) was found to have a similar effect on the separation selectivity of compounds **6–10** as observed for an increase in temperature. Trial-and-error adjustments yielded an optimal slope of 0.28% B/min following an isocratic hold period of 2 min at 10% B in the beginning to provide separation of compounds **1–12** within 19 min. The gradient steepness was subsequently increased to elute compounds **13–15** in an acceptable time, followed by a rinsing step with 100% B for 3 min (essential for the analysis of rooibos infusions). The optimised gradient provided minimum resolution of 1.25 and 0.92 for critical pairs **7/8** and **8/9**, respectively. A UV chromatogram (288 nm) for the optimised RP-LC separation of the phenolic standards is indicated in Fig. 5.

Preliminary validation of the optimised HPLC–DAD method was subsequently performed to demonstrate suitability for accurate quantitative analysis. Linearity of the calibration curves for standards over the studied concentration ranges was excellent, with correlation coefficients larger than 0.99997 and  $y$ -intercept values close to zero ( $\pm 1.9$  mAU). The stability of all phenolic compounds over a 27 h period ( $n=8$ ) was very good, with percentage relative standard deviation (% RSD) < 2%. Intraday ( $n=6$ ) and interday ( $n=3$ ) values were highly reproducible for all phenolic standards (% RSD < 5%).

### 3.3. Quantitative analysis of phenolic compounds in aqueous rooibos infusions

Although numerous HPLC methods suitable for the quantification of selected rooibos phenolics have been reported, the developed method is, to our knowledge, the first method suitable for the simultaneous quantification of these 15 phenolic compounds on conventional instrumentation. In our group, for example, two diverse methods (Section 2.4.5) were previously employed for the quantification of most of the compounds

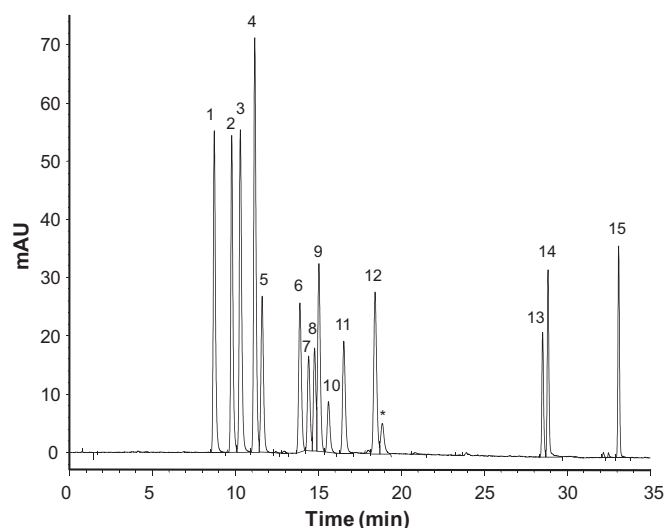


**Fig. 5.** UV chromatogram (288 nm) for the optimised RP-LC–UV separation of the phenolic standards on the 1.8  $\mu\text{m}$  Agilent Zorbax SB-C18 (100 mm  $\times$  4.6 mm) column at 37 °C. Peak labels correspond to Table 1. \* denotes a contaminant. For further experimental details, refer to Section 2.4.3.

(excluding isoquercitrin and ferulic acid, which could not be quantified due to co-elution). The first method was adapted from the HPLC method published by Joubert [7], initially developed for the quantification of the dihydrochalcones aspalathin and nothofagin in rooibos tea. This method [7] was transferred to a 5  $\mu\text{m}$  Gemini column (150 mm  $\times$  4.6 mm) and the solvent program adjusted to improve resolution on an Agilent 1200 HPLC system, leading to a run time of 90 min. The 2% formic acid aqueous solvent was also replaced with 2% acetic acid to simplify switching between methods. The adapted method was subsequently used for the quantification of vitexin, isovitexin, luteolin-7-*O*-glucoside, hyperoside, quercetin, luteolin and chrysoeriol. The second method employed in our group was a HPLC method of 23 min developed by Joubert et al. [6] for the rapid separation and quantification of aspalathin and its corresponding flavones, isoorientin and orientin, in fermented rooibos iced tea. This method was also deemed suitable for the quantification of PPAG, nothofagin and rutin.

The optimised HPLC–DAD method described in this paper was subsequently applied to the analysis of aqueous infusions of unfermented ( $n=10$ ) and fermented ( $n=10$ ) rooibos plant material. Quantitative data on the fermented samples were compared to those obtained for the identical samples using HPLC–DAD methods previously employed in our group. The mean content values of the major phenolic compounds, expressed as g per 100 g soluble solids, together with the standard deviations are summarised in Table 3.

The C-glycosyl dihydrochalcones aspalathin and nothofagin are, respectively, the most and second most abundant phenolic compounds present in unfermented rooibos infusions (Table 3). Despite its considerable decrease during fermentation, aspalathin remains one of the major phenolic constituents of fermented rooibos, while nothofagin is degraded to extremely low concentrations. These results are in agreement with previous reports [7] and indicate that C-glycosyl dihydrochalcones are not stable during the fermentation process. Conversely, the proportions of the other C-glycosyl flavonoids in unfermented rooibos were similar to those in fermented rooibos. It is important to emphasise that the fermented and unfermented rooibos did not originate from the same plant material and therefore differences in the content values could be attributed to factors other than the fermentation process, such as natural variation. Furthermore, even amongst the unfermented

**Table 3**

Mean content values (g per 100 g soluble solids  $\pm$  standard deviation) of the major phenolic compounds present in aqueous infusions of unfermented and fermented rooibos plant material.

Phenolic compound	Unfermented rooibos, $P_1$ ( $n = 5$ ) <sup>a</sup>	Unfermented rooibos, $P_2$ ( $n = 5$ ) <sup>a</sup>	Fermented rooibos ( $n = 10$ ) <sup>a</sup>	Fermented rooibos ( $n = 10$ ) <sup>a,b</sup>
PPAG	0.25 $\pm$ 0.051	0.44 $\pm$ 0.056	0.53 $\pm$ 0.10	0.60 $\pm$ 0.15
Isoorientin	0.72 $\pm$ 0.12	1.3 $\pm$ 0.16	1.3 $\pm$ 0.084	1.2 $\pm$ 0.16
Orientin	0.48 $\pm$ 0.080	0.81 $\pm$ 0.080	0.92 $\pm$ 0.053	0.92 $\pm$ 0.13
Aspalathin	8.4 $\pm$ 1.4	12.4 $\pm$ 1.0	0.64 $\pm$ 0.17	0.68 $\pm$ 0.19
Ferulic acid	nd <sup>d</sup>	nd <sup>d</sup>	0.088 $\pm$ 0.040	nq <sup>e</sup>
Quercetin-3- <i>O</i> -robinobioside <sup>c</sup>	0.43 $\pm$ 0.068	0.91 $\pm$ 0.12	0.94 $\pm$ 0.16	nd <sup>d</sup>
Vitexin	0.093 $\pm$ 0.015	0.18 $\pm$ 0.017	0.19 $\pm$ 0.016	0.18 $\pm$ 0.013
Hyperoside	0.046 $\pm$ 0.0079	0.18 $\pm$ 0.046	0.26 $\pm$ 0.076	0.26 $\pm$ 0.073
Rutin	0.30 $\pm$ 0.047	0.42 $\pm$ 0.018	0.23 $\pm$ 0.14	1.2 $\pm$ 0.30
Isovitexin	0.13 $\pm$ 0.021	0.23 $\pm$ 0.029	0.20 $\pm$ 0.017	0.21 $\pm$ 0.014
Isoquercitrin	0.090 $\pm$ 0.015	0.24 $\pm$ 0.038	0.18 $\pm$ 0.11	nq <sup>e</sup>
Nothofagin	0.69 $\pm$ 0.12	1.7 $\pm$ 0.16	0.10 $\pm$ 0.026	0.071 $\pm$ 0.013

<sup>a</sup> Mean content values (g compound per 100 g soluble solids).  $P_1$  and  $P_2$  refer to producers 1 and 2, respectively.

<sup>b</sup> Data for the same fermented samples, obtained using previous comparative HPLC methods.

<sup>c</sup> Quantified as rutin equivalents.

<sup>d</sup> nd, not detected.

<sup>e</sup> nq, not quantified due to coelution.

samples substantial variation was observed in the content values. The soluble solids of unfermented rooibos from producer 2 ( $P_2$ ) contained almost twice the amount of phenolic compounds compared to the unfermented rooibos supplied by producer 1 ( $P_1$ ). This was attributed to a more effective vacuum-drying process employed by producer 2, although natural variation could once again also be responsible for this observation.

Other major phenolic constituents of rooibos infusions include PPAG, isoorientin, orientin and a compound tentatively identified as quercetin-3-*O*-robinobioside (refer to LC-ESI-MS results in Section 3.4). The presence of PPAG, an enolic  $\beta$ -D-glucopyranoside of phenylpyruvic acid, in *A. linearis* plant material was first reported by Marais and co-workers in 1996 and identified using nuclear magnetic resonance (NMR) [30]. Luteolin-7-*O*-glucoside and the aglycones quercetin, luteolin and chrysoeriol were only present in trace amounts in both unfermented and fermented samples and could not be accurately quantified. Ferulic acid (not detected in unfermented rooibos) was present at low concentrations (0.088 g/100 g soluble solids) in fermented rooibos. Slight over-estimation of ferulic acid in some of the fermented samples was due to partial co-elution with an unknown compound (refer to LC-ESI-MS results in Section 3.4), present in low quantities.

The content values obtained using the optimised method are in good agreement with those obtained previously and, on average, only differs with ca.  $\pm$ 0.039 g compound/100 g soluble solids. The exception is rutin, for which the calculated content value is less than 20% of that obtained using the previous methods. This is due to perfect co-elution of rutin and the other quercetin-3-*O*-diglycoside, quercetin-3-*O*-robinobioside, in the previous method. These compounds exhibit identical UV and MS/MS spectra (Table 4), making it impossible to distinguish between them. This hypothesis is further supported by the combined content value of quercetin-3-*O*-robinobioside and rutin (1.2 g/100 g soluble solids), which is equal to the content value of rutin (1.2 g/100 g soluble solids) obtained using the previous method (Table 3). The high content values reported for rutin in other studies could also be overestimated for the same reason [8,9]. Stalmach et al. [3] and Kazuno et al. [11] have, however, discriminated between rutin and a rutin isomer and have reported individual content values for both compounds. It is assumed that the rutin isomer quantified in these reports [3,11] is in fact quercetin-3-*O*-robinobioside, which was identified in the current study by LC-MS and LC-MS/MS (see further). Comparison of previously reported content values to those obtained in the current study is difficult due to different sample preparation techniques. However, the higher relative concentration of the

isomer compared to rutin [3,11], is in agreement with our results for quercetin-3-*O*-robinobioside. Similar difficulties in the separation and quantification of the isomeric pair isoquercitrin and hyperoside have also been reported [8,9].

The developed HPLC-DAD method therefore demonstrated its suitability for the quantitative analysis of the principal phenolic constituents of rooibos. It is characterised by better resolution, higher sensitivity and shorter analysis times than previously reported methods and is therefore tailored for routine application. The method furthermore allowed us to report content values for PPAG, ferulic acid and quercetin-3-*O*-robinobioside in rooibos tea for the first time.

### 3.4. LC-ESI-MS and tandem MS analyses of aqueous rooibos infusions

LC-ESI-MS was used to confirm peak purity of the 15 standard phenolic compounds in aqueous rooibos infusions. In both unfermented and fermented rooibos samples, peak purity of the standards was established by comparison of MS spectra with reference compounds. The TOF-MS base peak chromatogram of a fermented rooibos infusion is depicted in Fig. 6. Note that LC-ESI-MS analyses were conducted on the Acquity UPLC system and in order to obtain equivalent separation [27] compared to the 1200 instrument the temperature was increased by 1 °C and the solvent preheated using an Acquity Column Stabilizer.

Identification of standard phenolic compounds (1–15) was based on comparison of  $t_R$ , UV-vis, MS and MS/MS data with those of authentic standards. The non-standard phenolic compounds (a–m) were tentatively identified by interpretation of UV and mass spectra in comparison with relevant literature reports. UV-vis spectrometry delimited the class of phenolic compounds [31], while accurate mass measurement and fragmentation patterns obtained by MS/MS were used to confirm the proposed structures. The nomenclature used here to describe the fragmentation is in accordance with [11,31,32], represented in Fig. 7 for a dihydrochalcone-C-6-hexoside. <sup>c,d</sup>X<sup>e+</sup> indicates the aglycone ion, where fragmentation on the carbohydrate ring is specified by the superscripts c and d. The position of glycosylation on the flavonoid A-ring (i.e. C-6 or C-8) is specified by the superscript e, and is similar for both positions (indicated only for the C-6 configuration in Fig. 7). For flavonoid-pentosides, additional characteristic losses of 60 *m/z* are common. Note that for high collision energies such as used here, additional loss of one or more water molecules were observed. For



**Table 4**  
Phenolic compounds identified in aqueous infusions of fermented and unfermented rooibos (*Aspalathus linearis*) by LC–ESI-MS and LC–ESI-MS/MS.

$t_R$ , min <sup>a</sup>	Peak	Negative		Positive				$\lambda_{max}$ , nm	Phenolic compound
		Accurate mass exp [M–H] <sup>–</sup>	Accurate mass exp [M+H] <sup>+</sup>	Accurate mass calc.	Proposed molecular formula	Error (ppm)	MS/MS fragment ions		
3.77	<b>a</b>	609.0861	611.1605	611.1612	C <sub>27</sub> H <sub>31</sub> O <sub>16</sub>	–1.1	425, 395 <sup>c</sup> , 365, 353, 341 <sup>c</sup>	230, 276, 340	Luteolin 6,8-di-C-hexoside
4.99	<b>b</b>	449.0543	451.1236	451.1240	C <sub>21</sub> H <sub>23</sub> O <sub>11</sub>	–0.9	231, 219, 195 <sup>c</sup> , 165	234, 287	(S)-eriodictyol-6-C-β-D-glucopyranoside
5.45	<b>c</b>	579.0714	581.1490	581.1506	C <sub>26</sub> H <sub>29</sub> O <sub>15</sub>	–2.8	425 <sup>c</sup> , 407 <sup>c</sup> , 395 <sup>c</sup> , 365, 353, 341	231, 273, 340	Carlinoside, isocarlinoside, neocarlinoside or isocarlinoside isomer
5.64	<b>d</b>	593.0682	595.1650	595.1663	C <sub>27</sub> H <sub>31</sub> O <sub>15</sub>	–2.2	457, 427, 409, 379 <sup>c</sup> , 355, 337, 325 <sup>c</sup>	231, 273, 331	Apigenin 6,8-di-C-hexoside (vicenin-2)
5.89	<b>e</b>	449.0450	451.1239	451.1240	C <sub>21</sub> H <sub>23</sub> O <sub>11</sub>	–0.2	231, 219, 195 <sup>c</sup> , 165	233, 288	(R)-eriodictyol-6-C-β-D-glucopyranoside
6.33	<b>f</b>	579.0608	581.1497	581.1506	C <sub>26</sub> H <sub>29</sub> O <sub>15</sub>	–1.5	425, 407, 395 <sup>c</sup> , 365, 353, 341	231, 273, 340	Carlinoside, isocarlinoside, neocarlinoside or isocarlinoside isomer
6.55	<b>g</b>	579.0819	581.1509	581.1506	C <sub>26</sub> H <sub>29</sub> O <sub>15</sub>	0.5	425 <sup>c</sup> , 407 <sup>c</sup> , 395 <sup>c</sup> , 365, 353, 341	233, 273, 340	Carlinoside, isocarlinoside, neocarlinoside or isocarlinoside isomer
6.81	<b>h</b>	449.0357	451.1238	451.1240	C <sub>21</sub> H <sub>23</sub> O <sub>11</sub>	–0.4	231, 219, 195 <sup>c</sup> , 165	233, 289	(S)-eriodictyol-8-C-β-D-glucopyranoside
7.23	<b>i</b>	449.0450	451.1242	451.1240	C <sub>21</sub> H <sub>23</sub> O <sub>11</sub>	0.4	231, 219, 195 <sup>c</sup> , 165	232, 289	(R)-eriodictyol-8-C-β-D-glucopyranoside
7.55	<b>j</b>	579.0714	581.1497	581.1506	C <sub>26</sub> H <sub>29</sub> O <sub>15</sub>	–1.5	425, 407, 395 <sup>c</sup> , 365, 353, 341	235, 276, 331	Carlinoside, isocarlinoside, neocarlinoside or isocarlinoside isomer
7.77	<b>1</b>	325.0378	327.1075	327.1080	C <sub>15</sub> H <sub>19</sub> O <sub>8</sub>	–1.5	119 <sup>c</sup> , 91	237, 280	Phenylpyruvic acid glucoside (PPAG)
8.70	<b>2</b>	447.0376	449.1088	449.1084	C <sub>21</sub> H <sub>21</sub> O <sub>11</sub>	0.9	329, 299 <sup>c</sup>	233, 270, 349	Luteolin-6-C-glucoside (isorientin)
9.15	<b>3</b>	447.0284	449.1083	449.1084	C <sub>21</sub> H <sub>21</sub> O <sub>11</sub>	–0.2	329 <sup>c</sup> , 299 <sup>c</sup>	236, 268, 348	Luteolin-8-C-glucoside (orientin)
9.92	<b>4</b>	451.0661	453.1401	453.1397	C <sub>21</sub> H <sub>25</sub> O <sub>11</sub>	0.9	247, 235, 205, 193, 165, 137, 123 <sup>c</sup>	235, 288	Aspalathin
10.28	<b>k</b>	613.1050	615.1929	615.1925	C <sub>27</sub> H <sub>35</sub> O <sub>16</sub>	0.7	435, 411, 369, 247, 235, 205, 193, 165 <sup>c</sup> , 137, 123	235, 288	8-C-hexosyl derivative of aspalathin
10.45	<b>5</b>	193.0039	195.0640	195.0657	C <sub>10</sub> H <sub>11</sub> O <sub>4</sub>	–8.7		239, 323	Ferulic acid
11.08	<b>l</b>	449.0450	451.1234	451.1240	C <sub>21</sub> H <sub>23</sub> O <sub>11</sub>	–1.3	379, 367, 325, 313, 301 <sup>c</sup> , 285, 271, 163	240, 287	Aspalalinin <sup>b</sup>
12.16	<b>m</b>	609.0969	611.1608	611.1612	C <sub>27</sub> H <sub>31</sub> O <sub>16</sub>	–0.7	303 <sup>c</sup>	256, 355	Quercetin-3-O-robinobioside
12.37	<b>6</b>	431.0317	433.1132	433.1135	C <sub>21</sub> H <sub>21</sub> O <sub>10</sub>	–0.7	313 <sup>c</sup> , 283 <sup>c</sup>	240, 269, 340	Apigenin-8-C-glucoside (vitexin)
12.89	<b>7</b>	463.0437	465.1024	465.1033	C <sub>21</sub> H <sub>21</sub> O <sub>12</sub>	–1.9	303 <sup>c</sup>	256, 355	Quercetin-3-O-galactoside (hyperoside)
13.21	<b>8</b>	609.9438	611.1613	611.1612	C <sub>27</sub> H <sub>31</sub> O <sub>16</sub>	0.2	303 <sup>c</sup>	256, 355	Quercetin-3-O-rutinoside (rutin)
13.47	<b>9</b>	431.0317	433.1135	433.1135	C <sub>21</sub> H <sub>21</sub> O <sub>10</sub>	0.0	313, 283 <sup>c</sup>	241, 271, 340	Apigenin-6-C-glucoside (isovitexin)
13.96	<b>10</b>	463.0155	465.1036	465.1033	C <sub>21</sub> H <sub>21</sub> O <sub>12</sub>	0.6	303 <sup>c</sup>	256, 355	Quercetin-3-O-glucoside (isoquercitrin)
14.81	<b>11</b>	447.0468	449.1078	449.1084	C <sub>21</sub> H <sub>21</sub> O <sub>11</sub>	–1.3	287 <sup>c</sup>	255, 348	Luteolin-7-O-glucoside
16.52	<b>12</b>	435.0605	437.1459	437.1448	C <sub>21</sub> H <sub>25</sub> O <sub>10</sub>	2.5	107 <sup>c</sup>	238, 287	Nothofagin
26.73	<b>13</b>	300.9807	303.0509	303.0505	C <sub>15</sub> H <sub>11</sub> O <sub>7</sub>	1.3		255, 371	Quercetin <sup>b</sup>
27.06	<b>14</b>	284.9890	287.0549	287.0556	C <sub>15</sub> H <sub>11</sub> O <sub>6</sub>	–0.7		253, 349	Luteolin <sup>b</sup>
31.28	<b>15</b>	299.0051	301.0719	301.0712	C <sub>16</sub> H <sub>13</sub> O <sub>6</sub>	2.3		250, 348	Chrysoeriol <sup>b</sup>

<sup>a</sup>  $t_R$  – retention time of the phenolic constituent in a fermented rooibos infusion.

<sup>b</sup> Only detected in fermented samples.

<sup>c</sup> Base peak(s) in the MS/MS spectrum.

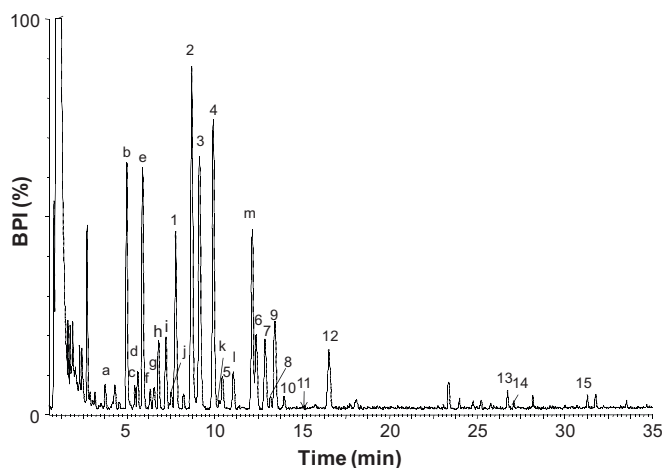


**Fig. 6.** Base peak chromatogram (acquired in negative ionisation mode) of a fermented rooibos infusion. Peak labels correspond to Table 4.

the specific case of dihydrochalcones,  $A^+$  and  $B^+$  denote charged fragments containing the A- and B-rings, respectively.

#### 3.4.1. Flavone di-C-glycosides

Peaks **c**, **f**, **g** and **j** with  $m/z$  581 ( $[M+H]^+$ ) were detected at retention times of 5.45, 6.33, 6.55 and 7.55 min, respectively, and had the same proposed molecular formula ( $C_{26}H_{29}O_{15}$ ). These compounds presented a major fragment ion at  $m/z$  395 corresponding to  $[M+H-150-2H_2O]^+$ . Compounds **c** and **g** additionally presented major fragment ions (intensities >90%) at  $m/z$  425 and  $m/z$  407, corresponding to losses of  $[M+H-120-2H_2O]^+$  and  $[M+H-120-3H_2O]^+$ , respectively. These fragments were also present in the MS/MS spectra of **f** and **j**, albeit at lower intensities (ca. 30%). These compounds exhibited identical UV spectra with maximum absorbance at ca. 230, 270 and 340 nm.

Based on similar results reported by Iswaldi and co-workers [5], three of these peaks were tentatively assigned as carlinside [33], neocarlinside [34] and isocarlinside [35]. Carlinside is a 6,8-di-C-glycoside of luteolin, with glucopyranosyl and arabinopyranosyl groups attached at the C-6 and C-8 positions, respectively. Neocarlinside differs from carlinside with regards to the arabinose configuration, while isocarlinside differs from carlinside in that the hexoside and pentoside moieties are attached at the C-8 and C-6 positions, respectively. The presence of luteolin-6-C-hexoside-8-C-pentoside (i.e. either carlinside or neocarlinside) in rooibos was recently proposed by Breiter et al. [4]. Iswaldi and co-workers

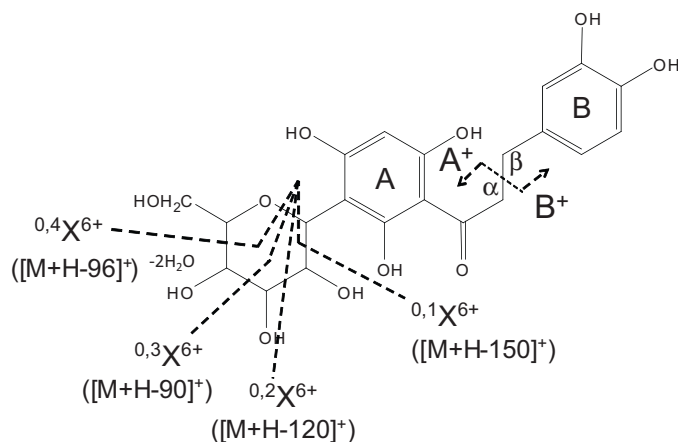


**Fig. 7.** General MS fragmentation pattern of flavonoid C-glycosides illustrated for the dihydrochalcone-C-6-glycoside aspalathin.

[5] tentatively identified a fourth peak with the same molecular ion as 2'-O- $\beta$ -arabinopyranosyl-orientin [33]. However, the four compounds **c**, **f**, **g** and **j** displayed similar MS/MS spectra which are consistent with asymmetric 6,8-di-C-glycosides of luteolin. We therefore propose that the fourth peak is more likely an isomer of the luteolin-6-C-pentoside-8-C-hexoside (isocarlinside), differing only with regard to the conformation of one of the sugar moieties.

Due to the absence of standards, it was impossible to distinguish between these isomers and allocate absolute peak identity. However, Abad-García et al. [32] showed that the relative ratio of the product ions  $[M+H-120]^+$  and  $[M+H-150]^+$  can be used to differentiate between flavone C-6- and C-8-mono-C-glycosides. For C-6-hexosides, ( $[M+H-150]^+/[M+H-120]^+$ ) yields a ratio of  $\sim 2$ , while for C-8-hexosides, this value is  $\sim 1$ . Extrapolation of this principle to flavone di-C-glycosides suggests that the hexoside is in the C-6 position for compounds **f** and **j** (ratio  $\sim 2$ ; luteolin-6-C-hexoside-8-C-pentoside, carlinside and neocarlinside). Accordingly, it is proposed that the hexoside is in the C-8 position for compounds **c** and **g** (ratio  $\sim 1$ ; luteolin-6-C-pentoside-8-C-hexoside, isocarlinside and an isomer).

Peak **a** ( $t_R=3.77$  min) exhibited pseudomolecular ions at  $m/z$  609 ( $[M-H]^-$ ) and  $m/z$  611 ( $[M+H]^+$ ) and maximum UV absorbance at  $\lambda=230, 276$  nm. Fragment ions of the protonated molecule were detected at  $m/z$  395 ( $[M+H-2\times 90-2H_2O]^+$ ) and 341 ( $[M+H-150-120]^+$ ). This fragmentation pattern, corresponding to losses of 90, 120 and 150 amu from the C-glycoside, was almost identical to those of **c**, **f**, **g** and **j** and compound **a** was therefore tentatively identified as another luteolin 6,8-di-C-glycoside. Due to the mass difference of 30 amu, it is proposed that peak **a** is a symmetric luteolin-di-C-hexoside. The presence of luteolin-6,8-di-C-hexoside in rooibos has been proposed by Breiter et al. [4].

Peak **d** ( $t_R=5.64$  min) with  $m/z$  593 ( $[M-H]^-$ ) and 595 ( $[M+H]^+$ ) and proposed molecular formula  $C_{27}H_{31}O_{15}$  ( $[M+H]^+$ ) was tentatively identified as the anti-inflammatory compound apigenin 6,8-di-C-glycoside, also known as vicenin-2. This compound showed a UV spectrum of a flavone derivative ( $\lambda_{max}$  at 273 and 331 nm), which is in line with  $\lambda_{max}$  values reported in [5,34]. Breiter et al. [4] and Iswaldi et al. [5] proposed the presence of this compound in rooibos, based on its occurrence in species such as *Viola vedoensis* MAKINO [34], *Citrus aurantifolia* [36] and *Lychnophora ericoides* Mart. [37]. The ESI-MS/MS spectrum of the protonated vicenin-2 molecule ( $m/z$  595,  $[M+H]^+$ ) showed the most abundant fragments at  $m/z$  379 and 325, with further fragments detected at  $m/z$  457, 427, 409 and 355 in accordance with [37].

#### 3.4.2. Flavanones

Peaks **b**, **e**, **h** and **i**, with  $m/z$  451 ( $[M+H]^+$ ) were detected at retention times of 4.99, 5.89, 6.81 and 7.23 min, respectively, and had the same proposed molecular formula ( $C_{21}H_{23}O_{11}$ ). The ESI-MS/MS spectra of the protonated compounds yielded major product ions at  $m/z$  195 and minor ions at  $m/z$  231, 219 and 165. These compounds exhibited identical UV response with maximum absorbance at ca. 233 and 288 nm. In accordance with literature, peaks **b** and **e**, and **h** and **i** were assigned as (S)- and (R)-eriodictyol-6-C- $\beta$ -D-glucopyranoside, and (S)- and (R)-eriodictyol-8-C- $\beta$ -D-glucopyranoside, respectively [8,38–40].

Koepfen and Roux postulated that these flavanone 6-C and 8-C compounds are formed as intermediates during the oxidative conversion of aspalathin to the flavones, isoorientin and orientin [41]. The presence of the 6-C-glycosides in fermented rooibos was unequivocally confirmed by Marais et al. [42], while NMR data for the 8-C-glycosides were presented by Krafczyk and Glomb in 2008 [39]. Eriodictyol-6-C- $\beta$ -D-glucopyranoside forms more readily than eriodictyol-8-C- $\beta$ -D-glucopyranoside, which results in a

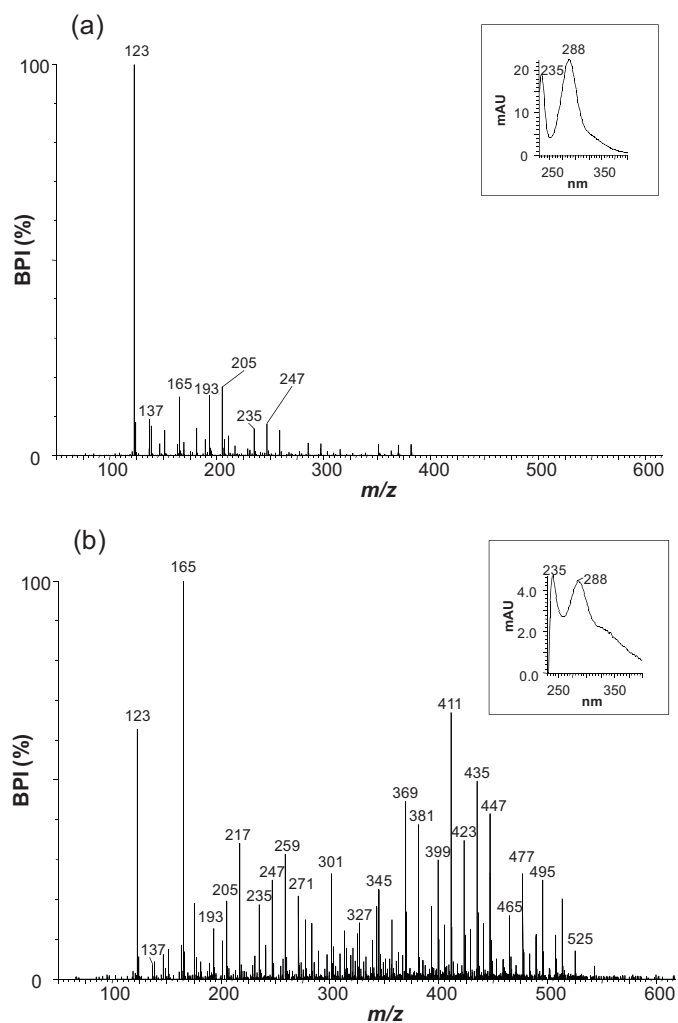


**Fig. 8.** MS/MS and UV spectra (insert) of (a) aspalathin and (b) unknown compound **k**.

ratio of ~2:1 for these compounds [39], as can be visualised by the relative ratios of **b** and **e** compared to **h** and **i** in Fig. 6.

#### 3.4.3. Dihydrochalcones

Compound **k**, eluting at 10.28 min, revealed molecular ions at  $m/z$  613 ( $[M-H]^-$ ) and  $m/z$  615 ( $[M+H]^+$ ). The experimental accurate mass (615.1929,  $[M+H]^+$ ) was in good accordance with the accurate mass calculated for the molecular formula  $C_{27}H_{35}O_{16}$ . Furthermore, UV and MS/MS spectra for compound **k** showed similar characteristics to those of aspalathin ( $m/z$  453,  $[M+H]^+$ ) (Fig. 8).

Due to the mass difference of 162 amu, compound **k** was proposed to be a glycosylated derivative of aspalathin. To confirm this hypothesis, analysis of the MS/MS spectra of these molecules was performed using the calculated molecular formulas for each fragment. The mass spectrum of aspalathin shows a base peak ion at  $m/z$  123 ( $C_7H_7O_2$ ), resulting from the cleavage of the bond between  $\alpha$ - and  $\beta$ -carbons ( $B^+$ , Fig. 7). Furthermore, related  $B^+$  fragments at  $m/z$  165 ( $C_9H_9O_3$ ) and 137 ( $C_8H_9O_2$ ), resulting from cleavage of the bonds on either side of the carbonyl group, were also observed for aspalathin. The same three ions were also present in the MS/MS spectrum of compound **k**, indicating that the B-ring is the same as for aspalathin, and therefore that the additional hexosyl residue is attached to the A-ring.

The fragment detected at  $m/z$  235 ( $[M+H-218]^+$ ,  $C_{12}H_{11}O_5$ ) for aspalathin results from  $^{0,4}X^+$  fragmentation of the C-glucose

and loss of two water molecules. Ions at  $m/z$  193 ( $[M+H-260]^+$ ,  $C_{10}H_9O_4$ ) result from  $^{0,2}X^+$  fragmentation of the C-glucose, followed by the loss of one water molecule. Similarly,  $m/z$  205 ( $[M+H-248]^+$ ,  $C_{11}H_9O_4$ ) results from  $^{0,3}X^+$  fragmentation of the C-glucose, followed by the loss of two water molecules. The ion detected at  $m/z$  247 ( $[M+H-206]^+$ ,  $C_{13}H_{11}O_5$ ) results from loss of the B-ring, followed by  $^{0,4}X^+$  fragmentation of the A<sup>+</sup> C-glucoside and loss of two water molecules. Significantly, fragments with  $m/z$  247, 235, 205 and 193 are all common to aspalathin and compound **k**, indicating that the latter also contains a C-6-hexoside functionality.

Finally, in the higher MW range, the MS/MS spectrum of compound **k** shows several ions consistent with a flavonoid C-6, C-8-dihexoside [37]:  $m/z$  525 ( $[M+H-90]^+$ ),  $m/z$  495 ( $[M+H-120]^+$ ),  $m/z$  477 ( $[M+H-120-H_2O]^+$ ),  $m/z$  465 ( $[M+H-150]^+$ ),  $m/z$  447 ( $[M+H-150-H_2O]^+$ ),  $m/z$  435 ( $[M+H-2 \times 90]^+$ ),  $m/z$  423 ( $[M+H-2 \times 96]^+$ ),  $m/z$  411 ( $[M+H-90-96-H_2O]^+$ ),  $m/z$  399 ( $[M+H-96-120]^+$ ),  $m/z$  381 ( $[M+H-96-120-H_2O]^+$ ),  $m/z$  369 ( $[M+H-96-150]^+$ ),  $m/z$  345 ( $[M+H-120-150]^+$ ) and  $m/z$  327 ( $[M+H-120-150-H_2O]^+$ ). The fragmentation pattern for this compound clearly corresponds with the simultaneous fragmentation of 2 C-hexosyl groups, as opposed to a C-6-dihexosyl (where the inter-sugar bond would preferentially be cleaved), or a O-hexoside (which would not result in cleavage within the second carbohydrate ring but rather loss of 162 amu).

These data lead us to propose that compound **k** is most likely the C-8-hexosyl derivative of aspalathin. This is to our knowledge the first time that this compound has been reported in literature. As a derivative of aspalathin, a compound unique to rooibos, it would be interesting to isolate this compound and study its chemical properties.

Peak **i** ( $t_R = 11.08$  min) with an accurate mass of  $m/z$  451.1234 ( $[M+H]^+$ , experimental) and the proposed molecular formula  $C_{21}H_{23}O_{11}$  ( $[M+H]^+$ ) was tentatively assigned to aspalalinin. The presence of this cyclic dihydrochalcone possessing an intramolecular ether linkage has been established in rooibos by NMR [38]. The ESI-MS/MS spectrum of the protonated aspalalinin molecule ( $m/z$  451,  $[M+H]^+$ ) showed the most abundant fragment at  $m/z$  301, which corresponds to  $[M+H-150]^+$ . Other fragments were found at  $m/z$  379, 367, 325, 313, 285, 271 and 163. This compound exhibited UV  $\lambda_{max}$  at 240 and 287 nm and was only detected in fermented rooibos.

#### 3.4.4. Flavonol O-glycosides

In contrast to flavonoid C-glycosides, the flavonol O-glycosides (compounds **7** and **10**, Table 4), and flavonol-3-O-dihexoside (compound **8**, Table 4) displayed much simpler MS/MS spectra, with the prevalent fragmentation involving cleavage at the glycosidic O-linkage. Rutin, quercetin-3-O-glucoside and quercetin-3-O-galactoside all showed only one fragment at  $m/z$  303, corresponding to the aglycone ion. A similar fragment was observed for compound **m** ( $t_R = 12.16$  min). ESI-MS showed a molecular ion similar to rutin at  $m/z$  611 ( $[M+H]^+$ ), while maximum UV absorbance at 256 and 355 nm was similar to that found for the other flavonol-O-glycosides (Table 4). Peak **m** was therefore tentatively identified as quercetin-3-O-robinobioside. The presence of this compound in rooibos has been unequivocally established by NMR [38]. This compound was also tentatively identified in rooibos by Iswaldi et al. [5], although the relative retention time and MS/MS spectra did not match our data, which are in agreement with other reports on this compound [4,43,44].

#### 3.4.5. Phenylpropanoid

PPAG (peak **1**,  $t_R = 7.77$  min) produced a protonated molecular ion at  $m/z$  327 ( $[M+H]^+$ ). The ESI-MS/MS spectrum of the protonated

compound showed a base peak at  $m/z$  119. This ion is likely formed as a result of cleavage of both the glucoside and carboxylic acid groups at C2. A second ion at  $m/z$  91 was presumably formed by the subsequent loss of formaldehyde resulting from cleavage of the C2–C3 bond.

#### 4. Conclusions

An HPLC–DAD method has been successfully developed for the quantitative determination of the 15 principal phenolic constituents of rooibos on conventional HPLC instrumentation. A systematic approach towards method development was used to optimise resolution on a selected sub-2  $\mu\text{m}$  column to exploit the benefits of this phase for fast analysis. Under the optimised gradient conditions and temperature, complete separation of the 15 principal phenolics could be obtained on a 1.8  $\mu\text{m}$  C18 phase within 37 min. This method was successfully applied to the quantitative analysis of aqueous infusions of fermented and unfermented rooibos. Quantitative data for ferulic acid, PPAG and quercetin-3-*O*-robinobioside are reported here for the first time.

Coupling of the optimised method to MS and tandem MS confirmed that no co-elution for the 15 target analytes occurred in fermented and unfermented rooibos infusions, and enabled the tentative identification of 13 additional phenolic constituents. These included 4 flavanones, a cyclic dihydrochalcone, and a flavonol-*O*-diglycoside previously reported in rooibos. The presence of the symmetric 6,8-di-*C*-glycosyl flavones (luteolin 6,8-di-*C*-hexoside and apigenin 6,8-di-*C*-hexoside) and the asymmetric 6,8-di-*C*-glycosyl flavones (carlinsoside, neocarlinsoside, isocarlinsoside) has been tentatively re-confirmed in this study. Based on MS/MS data, a fourth asymmetric di-*C*-glycosyl flavone is proposed to be an isomer of isocarlinsoside, differing only with regard to the sugar configuration. The presence of this compound in rooibos is reported here for the first time. Moreover, another phenolic compound (MW 614) is tentatively identified in rooibos for the first time, displaying structural characteristics in accordance with a *C*-8-hexosyl derivative of the dihydrochalcone aspalathin.

Establishment of this HPLC method will enable the comprehensive analysis of a cup of rooibos tea and the subsequent calculation of the contribution of rooibos polyphenols to dietary intake. Further application to a large number of samples would allow inclusion of data in food composition tables and provide typical fingerprints for product authenticity and quality control purposes. Future applications of the method will include authentication of extracts used in nutraceutical products on the basis of their flavonoid fingerprints; selection of plant material for propagation of genotypes producing high levels of specific phenolic markers; quantification of the effect of seasonal and geographical influences on composition; and correlating pharmacological activities with specific constituents.

#### Acknowledgements

The authors gratefully acknowledge the contribution of F. Lestremau for assistance with DryLab and M.A. Stander (Central Analytical Facility, Stellenbosch University) for assistance with LC–MS analyses. The National Research Foundation (NRF, South Africa, Grants 67143 to E. Joubert and 70995 to A. de Villiers), THRIP (Grant 72065 to E. Joubert) and SAAFoST FoodBev SETA are acknowledged for financial support.

#### Appendix A. Supplementary data

Supplementary data associated with this article can be found, in the online version, at doi:10.1016/j.chroma.2011.11.012.

#### References

- [1] E. Joubert, D. de Beer, S. Afr. J. Bot. 77 (2011) 869.
- [2] E. Joubert, W.C.A. Gelderblom, A. Louw, D. de Beer, J. Ethnopharmacol. 119 (2008) 376.
- [3] A. Stalmach, W. Mullen, M. Pecorari, M. Serafini, A. Crozier, J. Agric. Food Chem. 57 (2009) 7104.
- [4] T. Breiter, C. Laue, G. Kressel, S. Gröll, U.H. Engelhardt, A. Hahn, Food Chem. 128 (2011) 338.
- [5] I. Iswaldi, D. Arráez-Román, I. Rodríguez-Medina, R. Beltrán-Debón, J. Joven, A. Segura-Carretero, A. Fernández-Gutiérrez, Anal. Bioanal. Chem. 400 (2011) 3643.
- [6] E. Joubert, M. Viljoen, D. de Beer, M. Manley, J. Agric. Food Chem. 57 (2009) 4204.
- [7] E. Joubert, Food Chem. 55 (1996) 403.
- [8] L. Bramati, M. Minoggio, C. Gardana, P. Simonetti, P. Mauri, P. Pietta, J. Agric. Food Chem. 50 (2002) 5513.
- [9] L. Bramati, F. Aquilano, P. Pietta, J. Agric. Food Chem. 51 (2003) 7472.
- [10] H. Schulz, E. Joubert, W. Schütze, Eur. Food Res. Technol. 216 (2003) 539.
- [11] S. Kazuno, M. Yanagida, N. Shindo, K. Murayama, Anal. Biochem. 347 (2005) 182.
- [12] A. de Villiers, K.M. Kalili, M. Malan, J. Roodman, LCGC Eur. 23 (2010) 466.
- [13] D. Cabooter, K. Broeckhoven, K.M. Kalili, A. de Villiers, G. Desmet, J. Chromatogr. A 1218 (2011) 7347.
- [14] G. Desmet, D. Clicq, P. Qzil, Anal. Chem. 77 (2005) 4058.
- [15] D. Guillarme, S. Heinisch, J.L. Rocca, J. Chromatogr. A 1052 (2004) 39.
- [16] C.R. Wilke, P. Chang, AIChE J. 1 (1955) 264.
- [17] A. de Villiers, F. Lynen, P. Sandra, J. Chromatogr. A 1216 (2009) 3431.
- [18] G.A. Shabir, W.J. Lough, S.A. Arain, T.K. Bradshaw, J. Liq. Chromatogr. Rel. Technol. 30 (2007) 311.
- [19] A. de Villiers, F. Lestremau, R. Szucs, S. Gélébart, F. David, P. Sandra, J. Chromatogr. A 1127 (2006) 60.
- [20] J.M. Harnly, S. Bhagwat, L. Lin, Anal. Bioanal. Chem. 389 (2007) 47.
- [21] D. Cabooter, F. Lestremau, A. de Villiers, K. Broeckhoven, F. Lynen, P. Sandra, G. Desmet, J. Chromatogr. A 1216 (2009) 3895.
- [22] E. Oláh, S. Fekete, J. Fekete, K. Ganzler, J. Chromatogr. A 1217 (2010) 3642.
- [23] S. Fekete, K. Ganzler, J. Fekete, J. Pharm. Biomed. Anal. 54 (2011) 482.
- [24] G. Guiochon, J. Chromatogr. A 1126 (2006) 6.
- [25] P.L. Zhu, J.W. Dolan, L.R. Snyder, J. Chromatogr. A 756 (1996) 41.
- [26] W.S. Hancock, C. Rosanne, J.J. Chloupek, L.R. Kirkland, Snyder, J. Chromatogr. A 686 (1994) 31.
- [27] J.W. Dolan, J. Chromatogr. A 965 (2002) 195.
- [28] P. Jandera, J. Chromatogr. A 1126 (2006) 195.
- [29] J.W. Dolan, D.C. Lommen, L.R. Snyder, J. Chromatogr. 535 (1990) 55.
- [30] C. Marais, J.A. Steenkamp, D. Ferreira, Tetrahedron Lett. 37 (1996) 5763.
- [31] B. Abad-García, L.A. Berreuta, S. Garmón-Lobato, B. Gallo, F. Vicente, J. Chromatogr. A 1216 (2009) 5398.
- [32] B. Abad-García, S. Garmón-Lobato, L.A. Berreuta, B. Gallo, F. Vicente, Rapid Commun. Mass Spectrom. 22 (2008) 1834.
- [33] X. Li, Z. Xiong, X. Ying, L. Cui, W. Zhu, F. Li, Anal. Chim. Acta 580 (2006) 170.
- [34] C. Xie, N.C. Veitch, P.J. Houghton, M.S.J. Simmonds, Chem. Pharm. Bull. 51 (2003) 1204.
- [35] M.B.C. Gallo, W.C. Rocha, U.S. Da Cunha, F.A. Diogo, F.C. Da Silva, P.C. Vieira, J.D. Vendramim, J.B. Fernandes, M.F. das, G.F. Da Silva, L.G. Batista-Pereira, Pest Manage. Sci 62 (2006) 1072.
- [36] A.L. Piccinelli, M. García Mesa, D.M. Armenteros, M.A. Alfonso, A.C. Arevalo, L. Campone, L. Rastrelli, J. Agric. Food Chem. 56 (2008) 1574.
- [37] S.L. De Moraes, J.C. Tomaz, N.P. Lopes, Biomed. Chromatogr. 21 (2007) 925.
- [38] N. Shimamura, T. Miyase, K. Umehara, T. Warashina, S. Fujii, Biol. Pharm. Bull. 29 (2006) 1271.
- [39] N. Krafczyk, M.A. Glomb, J. Agric. Food Chem. 56 (2008) 3368.
- [40] C.S. Philbin, S.J. Schwartz, Phytochemistry 68 (2007) 1206.
- [41] B.H. Koepfen, D.G. Roux, Tetrahedron Lett. 39 (1965) 3497.
- [42] C. Marais, W.J. Van Rensburg, D. Ferreira, J.A. Steenkamp, Phytochemistry 55 (2000) 43.
- [43] J.A. Ozga, A. Saeed, W. Wismer, D.M. Reinecke, J. Agric. Food Chem. 55 (2007) 10414.
- [44] L.-Z. Lin, P. Chen, J.M. Harnly, J. Agric. Food Chem. 56 (2008) 8130.